

ОБЪЕДИНЕННЫЙ
ИНСТИТУТ
ЯДЕРНЫХ
ИССЛЕДОВАНИЙ
ДУБНА

К 74

E2-87-548

B.Z.Kopeliovich, B.G.Zakharov*

**$\bar{p}p$ ANNIHILATION
IN THE DUAL PARTON MODEL
AND PERTURBATIVE QCD**

Submitted to "Ядерная физика"

* Institute of Terrestrial Physics,
Academy of Sciences of the USSR

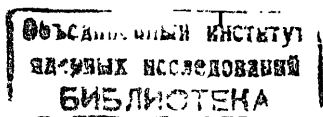
1987

1. INTRODUCTION

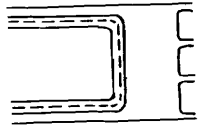
Experimental data on high-energy hadronic interaction have been successfully described in the quark-gluon string model (SM)^{/1-8/} in the last years. SM is based on the idea of topological expansion (TE)^{/9/}, which is equivalent to the $1/N_F$ expansion in QCD with $N_F/N_c = \text{const}$ ^{/10/}. The Reggeon exchange corresponds to the planar diagram, but the Pomeron exchange is described by the cylinder-type diagram. It is also assumed in the SM that hadrons are produced as a result of disintegration of colour strings formed due to confinement after colour exchange in hadronic collision^{/11-13/}. The cut of the planar reggeon graph of TE corresponds in the SM to annihilation of valence $q\bar{q}$ -pair followed by formation of colour string by a pair of spectator quarks. The cut of the cylindrical graph of TE contains two $q\bar{q}$ -strings which decay independently in the leading $1/N$ approximation.

The TE for the reaction with baryons has no foundation. Nevertheless a pair of quarks (called diquark D) in the colour $\bar{3}$ -state is considered in the SM analogously to \bar{q} in a meson. But this approach is not valid in the case of $p\bar{p}$ annihilation if it is accompanied by destruction of diquarks.

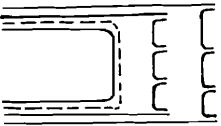
Rossi and Veneziano^{/15/} have proposed to associate $p\bar{p}$ annihilation at high energies with annihilation of string junctions (SJ) as is shown in Fig.1 (SJ is denoted by the dashed line). The concept of SJ has naturally appeared in the gauge-invariant representation of wave function (WF) of the nucleon^{/15,16/}. In the string model SJ is point where strings are connected together^{/17/} if the baryon has a form of Y. Unfortunately, this qualitative pattern is not supplied with any calculation scheme. From the SM point of view graphs in Fig.1 a,b,c correspond to formation, in the final state, of one, two or three $q\bar{q}$ -strings. These strings mainly decay into meson states because produc-



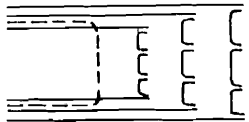
tion of $D\bar{D}$ pairs is suppressed. One can see that the diquark can be treated as a colour triplet only in the case of graph in Fig.1a.



a



b



c

Fig.1

Here $\alpha_B(0)$ is the baryon trajectory intercept; g is reggeon-particle coupling constant which is connected through bootstrap condition with the secondary reggeon intercept^{/19,20/}: $\alpha_M(0) = 2\alpha_B(0) - 1 + g^2$.

If $\alpha_M(0) = 0.5$, $\alpha_B(0) = 0$, then^{/18/}

$$\alpha_{M_4^J}(0) = -0.5, \quad \alpha_{M_2^J}(0) = 0, \quad \alpha_{M_0^J}(0) = 0.5.$$

These results of paper^{/18/} lead to a wide spread opinion that the experimentally observed energy dependence of annihilation cross section $\sigma_{ann}^{PP} \propto E^{-2}$ corresponds to the contribution of the three-sheet graph in Fig.1 c, and that this energy region ($E < 12$ GeV) is an asymptotical one^{/1,5,6,15,16,22-24/}. But the Chew-Pignotti model is obviously oversimplified, the multiperipheral model is too crude, thus more profound investigation of contributions to σ_{ann} of graphs in Fig.1 is needed.

From the point of view of unitarity diagrams in Fig.1 a,b,c correspond to contributions of Regge trajectories M_4^J , M_2^J and M_0^J (notation of ref.^{/16/}) to the elastic scattering amplitude. Eilon and Harrari^{/18/} gave the first estimation of the intercepts of these trajectories before the conception of SJ had been introduced. Using the Chew-Pignotti approach^{/21/} to the dual multiperipheral model^{/19,20/} they obtained

$$\alpha_{M_4^J}(0) = 2\alpha_B(0) - 1 + g^2 \quad (1)$$

$$\alpha_{M_2^J}(0) = 2\alpha_B(0) - 1 + 2g^2 \quad (2)$$

$$\alpha_{M_0^J}(0) = 2\alpha_B(0) - 1 + 3g^2 \quad (3)$$

Below we consider a natural mechanism in the QCD perturbative theory (PT) leading to the three-sheet configuration of the type shown in Fig.1 c. It can be a result of exchange by two gluons in the decuplet colour state^{/25/} (see Fig.2). $(3q)_{\{10\}}(3\bar{q})_{\{10\}}$ final state can be considered as three $q\bar{q}$ colourless states independently decaying into hadrons (in the SM). The last stage is not described in PT of course. As the strings decay with a unit probability one can consider the

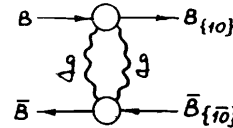


Fig.2

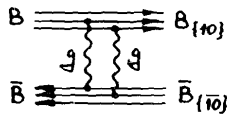
cross section of the process $B\bar{B} \rightarrow (3q)_{\{10\}}(3\bar{q})_{\{10\}}$ (denoted below $\sigma_{\{10\}}$) calculated in PT to be equal to the cross section for three-sheet events. It is clear that in the lowest order approximation this cross section is energy independent.

It is interesting that $\sigma_{\{10\}}$ is sensitive to the minimal distance between any pair of quarks in the baryon and $\sigma_{\{10\}} \rightarrow 0$ in this distance tends to zero. This is the result of colour screening. The spatial part of the three-quark decuplet state is antisymmetrical so the value of $\sigma_{\{10\}}$ is determined by gluon momenta of about inverse minimal distance between quarks. This leads to more appropriate conditions for PT validity than in the case of σ_{tot} calculation in the double gluon approximation^{/11,26,27/}, where gluon momenta of about inverse hadron radius are essential. Strong dependence of $\sigma_{\{10\}}$ on the minimal interquark distance is especially important for $N\bar{N}$ -annihilation if the nucleon contains the diquark of a small radius. Such possibility is justified by calculations^{/28/} in the instanton vacuum, by analysis of deep inelastic reactions^{/29-32/} and large p_T processes^{/33-36/}.

The paper is organized as follows. The formulae for $\sigma_{\{10\}}$ calculation are obtained in Section 2. Section 3 contains the results of numerical calculation. In Section 4 this results are discussed and compared with the experimental data and with the dual topological approach.

2. FORMULAE FOR $\sigma_{\{10\}}$

The colour wave functions (WF) of baryons in the initial state (Fig.2) are antisymmetrical but they are symmetrical in the final state. Thus the problem is reduced to calculation of the diagrams of the type shown in Fig.3. The corresponding cross section can be written in the following form:



$$\sigma_{\{10\}} = \frac{\alpha_s^4}{256\pi^2} \int \prod_{i=1}^4 \frac{d^2 q_i}{(q_i^2 + M_g^2)} \delta^{(2)}\left(\sum_{j=1}^4 \vec{q}_j\right) \times$$

$$\sum_{\alpha_1, \dots, \alpha_4=1}^8 R^{\alpha_1, \dots, \alpha_4}(q_1, \dots, q_4) \times$$

$$\bar{R}^{\alpha_1, \dots, \alpha_4}(q_1, \dots, q_4), \quad (4)$$

where

$$R^{\alpha_1, \dots, \alpha_4}(q_1, \dots, q_4) = \sum_{\substack{i_1 \neq i_2 \\ i_3 \neq i_4}} \sum_{\{10\}} \langle \Psi_{STR}^+ \Psi_C^{\{1\}} | \hat{\lambda}_{i_1}^{\alpha_1} \hat{\lambda}_{i_2}^{\alpha_2} \times$$

$$\exp(i\vec{q}_1 \vec{z}_{i_1} + i\vec{q}_2 \vec{z}_{i_2}) | \Psi_{STR}^- \Psi_C^{\{10\}} \rangle \times$$

$$\langle \Psi_{STR}^- \Psi_C^{\{10\}} | \hat{\lambda}_{i_3}^{\alpha_3} \hat{\lambda}_{i_4}^{\alpha_4} \exp(i\vec{q}_3 \vec{z}_{i_3} + i\vec{q}_4 \vec{z}_{i_4}) | \Psi_{STR}^+ \Psi_C^{\{1\}} \rangle. \quad (5)$$

Here M_g is the gluon mass which effectively takes into account the confinement; $\hat{\lambda}^\alpha$ are the Gell-Mann colour matrices; α_s is the QCD coupling constant; Ψ_{STR}^+ and Ψ_{STR}^- are the three-quark WFs, depending on spin, isotospin and spatial coordinates with the Young schemes $\square\square$ and \square , respectively; $\Psi_C^{\{1\}}$ and $\Psi_C^{\{10\}}$ are the single and decuplet colour WFs; \vec{z}_i are the spatial coordinates of quarks in the three-quark c.m.; \vec{q}_i are the gluon transverse momenta. The indices

i_1, \dots, i_4 - number the quarks in the three-quark WF; the sum over $\{10\}$ denotes the sum over all possible states of three quarks which are in the decuplet colour state. The expression for $\bar{R}^{\alpha_1, \dots, \alpha_4}$ in formula (4) differs from (5) by substitution of $\hat{\lambda}^\alpha \rightarrow (\hat{\lambda}^\alpha)^T$. Due to symmetry of all expressions in the brackets in formula (5) one can replace the sum over Ψ_{STR}^+ by the sum over Ψ_{STR} with any Young scheme of three-quark system. Then (5) can be rewritten as follows

$$R^{\alpha_1, \dots, \alpha_4}(q_1, \dots, q_4) = \sum_{\substack{i_1 \neq i_2 \\ i_3 \neq i_4}} \langle \Psi_{STR}^+ | \exp(i \sum_k \vec{q}_k \vec{z}_{i_k}) | \Psi_{STR}^+ \rangle \times$$

$$\sum_{\{10\}} \langle \Psi_C^{\{1\}} | \hat{\lambda}_{i_1}^{\alpha_1} \hat{\lambda}_{i_2}^{\alpha_2} | \Psi_C^{\{10\}} \rangle \langle \Psi_C^{\{10\}} | \hat{\lambda}_{i_3}^{\alpha_3} \hat{\lambda}_{i_4}^{\alpha_4} | \Psi_C^{\{1\}} \rangle. \quad (6)$$

Using symmetry of $\Psi_C^{\{1\}}$ and antisymmetry of $\Psi_C^{\{10\}}$ one can represent (6) in the form

$$R^{\alpha_1, \dots, \alpha_4}(q_1, \dots, q_4) = 6R(q_1, \dots, q_4) C^{\alpha_1, \dots, \alpha_4}, \quad (7)$$

where

$$C^{\alpha_1, \dots, \alpha_4} = \sum_{\{10\}} \langle \Psi_C^{\{1\}} | \hat{\lambda}_1^{\alpha_1} \hat{\lambda}_2^{\alpha_2} | \Psi_C^{\{10\}} \rangle \langle \Psi_C^{\{10\}} | \hat{\lambda}_3^{\alpha_3} \hat{\lambda}_4^{\alpha_4} | \Psi_C^{\{1\}} \rangle, \quad (8)$$

$$R(\vec{q}_1, \dots, \vec{q}_4) = F(\vec{q}_1 + \vec{q}_3, \vec{q}_2 + \vec{q}_4, 0) + F(\vec{q}_1 + \vec{q}_4, \vec{q}_2, \vec{q}_3) +$$

$$F(\vec{q}_1, \vec{q}_2 + \vec{q}_3, \vec{q}_4) - F(\vec{q}_1 + \vec{q}_4, \vec{q}_2 + \vec{q}_3, 0) - F(\vec{q}_1 + \vec{q}_3, \vec{q}_2, \vec{q}_4) -$$

$$F(\vec{q}_1, \vec{q}_2 + \vec{q}_4, \vec{q}_3). \quad (9)$$

Here

$$F(\vec{q}_1, \vec{q}_2, \vec{q}_3) = \langle \Psi_{STR}^+ | \exp(i \sum_{i=1}^3 \vec{q}_i \vec{z}_i) | \Psi_{STR}^+ \rangle \quad (10)$$

is the three-particle formfactor.

The same formulae (7)-(10) are valid for $\bar{R}^{\alpha_1 \dots \alpha_4}(q_1, \dots, q_4)$ after substitution of $\hat{\lambda}^\alpha \rightarrow (\hat{\lambda}^\alpha)^\top$ in (8).

It is seen that expression (9) vanishes if any of gluon momenta tends to zero. This provides infrared stability of $\bar{O}_{\{10\}}$. Using (9) one can see that $R(q_1, \dots, q_4)$ also vanishes if the mean internal distance for any quark pair tends to zero.

The colour factor

$$C = \sum_{\alpha_1, \dots, \alpha_4=1}^8 C^{\alpha_1, \dots, \alpha_4} \bar{C}^{\alpha_1, \dots, \alpha_4} \quad (11)$$

is calculated in the appendix and is equal to $C = 160/9$. Using this value and expressions (4), (7) one can write $\bar{O}_{\{10\}}$ in the form

$$\bar{O}_{\{10\}} = \frac{5\alpha_s^4}{2\pi^2} \int \prod_{i=1}^4 \frac{d^2 q_i}{(q_i^2 + M_q^2)} \delta^{(2)}\left(\sum_{j=1}^4 \vec{q}_j\right) R^2(q_1, \dots, q_4). \quad (12)$$

Let us use two types of the nonrelativistic nucleon WF to calculate $\bar{O}_{\{10\}}$ in $\bar{N}\bar{N}$ collision. In the first case (denoted by I) we use the symmetrical oscillatory spatial WF, for which

$$F(\vec{Q}_1, \vec{Q}_2, \vec{Q}_3) = \exp\left\{-\frac{\langle \tau_p^2 \rangle}{6} [\vec{Q}_1^2 + \vec{Q}_2^2 + \vec{Q}_3^2 - \vec{Q}_1 \vec{Q}_2 - \vec{Q}_1 \vec{Q}_3 - \vec{Q}_2 \vec{Q}_3]\right\}, \quad (13)$$

where $\langle \tau_p^2 \rangle$ is the proton mean squares radius.

In the second case we take into account the possibility^{/28,30-36/} that the compact ud -diquark with $S=T=0$ is dynamically enhanced in the nucleon WF. The WF Ψ_{STR}^+ is written in this case as

$$(\Psi_{STR}^+)^{\bar{11}} = A (\Psi_{1,23} + \Psi_{2,31} + \Psi_{3,12}). \quad (14)$$

Here A is the normalization factor; $\Psi_{i,jk}$ is the three-quark WF with the quarks j, k in the state $S=T=0$. The spatial part of $\Psi_{i,jk}$ is taken in the form

$$\Psi_{i,jk}(\tau_1, \dots, \tau_3) = \left(\frac{2\alpha}{\pi}\right)^{\frac{3}{2}} \left(\frac{2\beta}{\pi}\right)^{\frac{3}{2}} \exp(-\alpha\rho^2 - \beta\tau^2), \quad (15)$$

where $\vec{\rho} = \vec{\tau}_i + (\vec{\tau}_j + \vec{\tau}_k)/2$; $\vec{\tau} = \vec{\tau}_j - \vec{\tau}_k$.

Calculating $F_{II}(Q_1, Q_2, Q_3)$ we neglect the interference terms of type $\langle \Psi_{1,23} | \exp(i \sum_{i=1}^3 \vec{Q}_i \cdot \vec{\tau}_i) | \Psi_{2,31} \rangle$ and $\langle \Psi_{2,31} | \Psi_{1,23} \rangle$. It can be justified by spin-isospin suppression of the interference terms by the factor 1/2, and by a small value of the spatial overlap integral in the case of the compact diquark.

The values of parameters α, β in (15) are related to the mean squared radius of the proton $\langle \tau_p^2 \rangle$ and the diquark $\langle \tau_D^2 \rangle$.

$$\alpha = \frac{2\varepsilon^2 + (1-\varepsilon)^2}{4\langle \tau_p^2 \rangle (1 - \langle \tau_D^2 \rangle / 3\langle \tau_p^2 \rangle)}; \quad \varepsilon = \frac{m_D}{m_q + m_p}; \quad \beta = \frac{3}{16\langle \tau_D^2 \rangle}. \quad (16)$$

WF (4), (5) leads to the following expression for the formfactor

$$F_{II}(Q_1, Q_2, Q_3) = \frac{1}{3} (F_{1,23} + F_{2,31} + F_{3,12}), \quad (17)$$

where

$$F_{i,jk} = \exp\left\{-\frac{1}{8\alpha} [\varepsilon \vec{Q}_i + (1-\varepsilon)(\vec{Q}_j + \vec{Q}_k)]^2 - \frac{(\vec{Q}_j - \vec{Q}_k)^2}{32\beta}\right\}. \quad (18)$$

It is worth noting that results of fitting of baryon Regge trajectories in the string^{/3,7/} and estimation in the instanton vacuum model^{/28/} show that the scalar diquark has a mass about 0.2 GeV, i.e. even smaller than the constituent quark mass ~ 0.3 GeV. Thus the use of the nonrelativistic approximation for the quark WF as a bound state of the quark with a mass ~ 0.3 GeV and the diquark with a mass ~ 0.2 GeV is of course unjustified. Formulae (17), (18) are the convenient parametrization taking into account small size of the diquark.

Evidently, higher order corrections do not drastically change the energy dependence of $\bar{O}_{\{10\}}$. It is shown in paper^{/38/} that in the leading logarithmic approximation exchange of two reggeized gluons in decuplet colour state corresponds to the Regge trajectory intercept $\alpha_{\{10\}}(0) = 1 - 3\alpha_s / 2\pi$. One can fix the value of α_s of the pomeron comparing the results of the leading logarithmic approximation^{/39/} for

the Pomeron intercept $\alpha_P(0) - 1 = 12 \ln 2 \alpha_s / \pi$ and the fit^[40] of the experimental data $\alpha_P(0) - 1 \approx 0.3$. Then one obtains $\alpha_{\{10\}}(0) - 1 \approx -0.05$.

3. RESULTS OF CALCULATIONS

The following procedure has been used to determine the value of α_s . First the experimental value of the total cross section $\sigma_{tot}^{NN} \approx 39$ mb is compared with the results of the Born approximation

$$(\sigma_{tot}^{NN})^I = 8\pi \alpha_s^2 J(\frac{\langle \tau_D^2 \rangle}{2}, \frac{\langle \tau_D^2 \rangle}{2}, M_g^2) \quad (19)$$

or with

$$(\sigma_{tot}^{NN})^{II} = \frac{8\pi \alpha_s^2}{9} [4J(a, a, M_g^2) + 4J(a, b, M_g^2) + J(b, b, M_g^2)]. \quad (20)$$

where $a = 1/8\alpha + 1/32\beta$;
 $b = 1/8\beta$;
 $J(x, y, z) = \int_0^\infty dt \frac{(1 - e^{-xt})(1 - e^{-yt})}{(t+z)^2}$.
 We fix here $\langle \tau_D^2 \rangle = 0.8$ Fm; $M_g = m_\pi$. This value of α_s is denoted below by the index {8}. The value of α_s for the diagram in Fig.3 is related to $\alpha_s^{\{8\}}$ through the one-loop approximation formula

$$\alpha_s^{\{10\}} = \alpha_s^{\{8\}} \ln(\langle q \rangle_{\{10\}} / \Lambda) / \ln(\langle q \rangle_{\{8\}} / \Lambda). \quad (21)$$

Here $\langle q \rangle_{\{8\}}$, $\langle q \rangle_{\{10\}}$ are the mean gluon transverse momenta obtained from formulae (19), (20) and (12), respectively. The QCD parameter Λ is fixed by expression $\alpha_s^{\{8\}} = 6\pi(33 - 2N_F)^{-1} \ln^{-1}(\langle q \rangle_{\{8\}} / \Lambda)$.

To determine $\langle q \rangle_{\{8\}}$, $\{10\}$ we use two methods: i) straightforward calculation of $\langle q \rangle$; ii) determination of the "mean momentum" from the result of averaging of $\langle \ln q \rangle$. The curves for $\langle q \rangle$ obtained by the first method are shown in Fig.4. The second variant leads to smaller values of $\langle q \rangle$. Nevertheless difference between two variants

for $\alpha_s^{\{10\}}$ which are shown in Fig.5 is negligibly small.

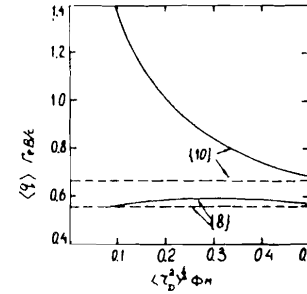


Fig.4. Value of $\langle q \rangle$ -mean transverse gluon momentum depending on the diquark radius $\langle \tau_D^2 \rangle^{1/2}$. Dashed lines show values of $\langle q \rangle$ obtained in variant I: $|p\rangle = |\text{und}\rangle$. Signs 8 and 10 denote calculations of $\langle q \rangle$ for σ_{tot} and $\sigma_{\{10\}}$.

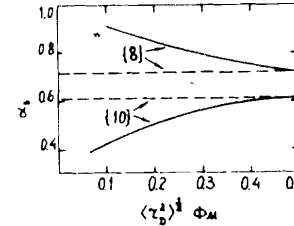


Fig.5. Mean values of α_s . Solid and dashed curves correspond to variants II and I.

Using these values of α_s one obtains the cross section $\sigma_{\{10\}}$ which is shown in Fig.6 as function of the diquark size $\langle \tau_D^2 \rangle^{1/2}$ (in variant II).

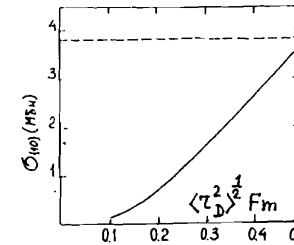


Fig.6. Values of $\sigma_{\{10\}}$ calculated in variants II (solid curve) and I (dashed line).

It is seen that $\sigma_{\{10\}}^I \approx \sigma_{\{10\}}^{II} \approx 2$ mb if $\langle \tau_D^2 \rangle^{1/2} \approx 0.6$ Fm, but when $\langle \tau_D^2 \rangle$ decreases, $\sigma_{\{10\}}^{II}$ falls due to diminution of integral in (12). In addition, a decrease of $\langle \tau_D^2 \rangle$ causes an increase of $\langle q \rangle$, which leads to smaller α_s . Note that in spite of neglecting the interference, the results of both variants $\sigma_{\{10\}}$ and $\sigma_{\{10\}}$ are close in value if $\langle \tau_D^2 \rangle^{1/2} \approx \sqrt{3}/2 \langle \tau_D^2 \rangle^{1/2}$. This confirms smallness of interference terms.

We also investigate sensitivity of $\sigma_{\{10\}}$ to some parameters. If one fixes $M_q = 0$, the absolute value of $\sigma_{\{10\}}$ falls by about 20-30% in comparison with Fig. 6. We also calculate $\sigma_{\{10\}}^I$ with $\langle r_p^2 \rangle^{1/2} = 0.7 \text{ fm}$ and $\sigma_{\{10\}}^{\bar{I}}$ with $m_D = 2 m_q$. The cross section changes within 30-60%. Thus we conclude that our predictions have uncertainty up to about factor 2.

The value of $\sigma_{\{10\}}$ determines the cross section of three-jet events. To obtain contribution to the annihilation cross section $\sigma_{ann}^{B\bar{B}}$, one should multiply $\sigma_{\{10\}}$ by a factor $\exp[-3\langle n_\pi \rangle w_N/w_\pi]$, where w_N/w_π is the ratio of nucleon-to-pion production probabilities in the central rapidity region, $w_N/w_\pi \approx 0.03$ in the FNAL-ISR energy interval; $\langle n_\pi \rangle \approx 2 \ln(s/s_0)$ is the mean multiplicity of pions.

4. DISCUSSION OF THE RESULTS

Unfortunately, there are experimental data on the annihilation cross section^{/23/} $\sigma_{ann}^{P\bar{P}}$ only up to 12 GeV. It is now impossible to extract the energy independent contribution (about 1 - 2 mb) we are interested in from the data in such a narrow energy interval. The experimentally measured cross section falls with energy approximately as $s^{-0.5}$. Some justification of our results comes from comparison of pp and p \bar{p} ISR data^{/38/}. The inclusive cross section of particle production in the central region in the p \bar{p} interaction is about 3 - 5% higher than in the pp one^{/41/}. This value is in agreement with the above estimate of the cross section for three-jet events if one assumes that nonannihilation multi-jet events in p \bar{p} and pp collisions have the same cross section. The data on topological cross section difference in p \bar{p} and pp collision $\Delta\sigma_n = \sigma_n^{P\bar{P}} - \sigma_n^{PP}$ at ISR energy^{/41/} have too large errors to draw definite conclusions. Nevertheless, one can see that $\Delta\sigma_n$ is concentrated at $n > \langle n_{pp} \rangle$. The cross section of such events $\sum_{n > \langle n \rangle} \Delta\sigma_n \approx 1 - 2 \text{ mb}$. This value is in agreement with our estimation of the three-jet production

cross section. Nevertheless this conclusion requires stronger statistical justification.

Besides the weak energy dependence of the three-jet cross section the colour-decuplet gluonic exchange is characterized by considerable quark transverse momenta on the string ends. These momenta are determined by transverse momenta of gluons and incident quarks, which are both determined by the inverse diquark radius (see Fig. 4). Thus transverse momenta of the ends of the strings are about 0.8-1.2 GeV/c. This is displayed in a fast growth of mean transverse momenta of produced particles with increasing X_F . A similar sea-gull effect is known in nonannihilation processes^{/8/}, but it is much weaker there.

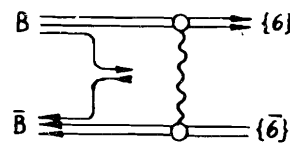


Fig. 7.

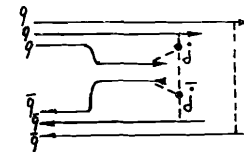


Fig. 8.

Let us now consider the contribution to σ_{ann} , which has energy dependence $s^{-0.5}$ within the framework of SM. It can be related to the graph shown in Fig. 7. It is assumed that each colliding particle contains at least one slow valence quark and pair of $q\bar{q}$ has small effective mass $M_{q\bar{q}} \lesssim 1 \text{ GeV}$. The gluonic exchange leads to transition of the diquarks D and \bar{D} into sextets $\{6\}$ and $\{6\bar{6}\}$ correspondingly. From the point of view of SM this results in the final state string configuration shown in Fig. 8 (the dashed lines denote the colour strings). If effective mass of the $q\bar{q}$ -pair is sufficiently small, $M_{q\bar{q}} \lesssim 1 \text{ GeV}$, then this string configuration can decay into mesons only.

Diagram analogous to one shown in Fig. 7 gives contribution to pp-scattering also. It describes the events with $q\bar{q}$ pair production

in the central rapidity region. These diagrams give the same contribution to the pp and $\bar{p}p$ total cross sections. This corresponds to the Eilon-Harrari hypothesis ^{/18/}, that annihilation contributes to the Pomeron.

It is possible also annihilation mechanism analogous to one shown in Fig. 7 but with $\bar{q}q$ -pair annihilation. Its contribution to annihilation cross section also drops with energy as $S^{-1/2}$. From the unitarity point of view this is nonplanar contribution to the ω -Reggeon.

Both mechanisms shown in Fig. 7 and gluonic colour decuplet exchange are characterized by high transverse momenta of string ends $\sim 1/\tau_D$. It has been noted above that this leads to a considerable sea-gull effect which is actually seen in the $p\bar{p}$ annihilation data at energies $\sqrt{s}_{lab} \approx 12$ GeV. At the same time the sea-gull effect in nonannihilation events is much weaker ^{/23/} and maximal values of $\langle p_T \rangle$ are about $0.3 + 0.4$ GeV/c.

An additional check of the proposed mechanism is possible if one investigates long rapidity correlations of transverse momenta of produced particles.

APPENDIX

Using the relation

$$\sum_{\{10\}} \langle i_1 i_2 i_3 | \Psi_c^{\{10\}} \rangle \langle \Psi_c^{\{10\}} | j_1 j_2 j_3 \rangle = \frac{1}{6} \{ \delta_{j_1}^{i_1} \delta_{j_2}^{i_2} \delta_{j_3}^{i_3} + (\text{permut. } j_1, j_2, j_3) \}.$$

where i, j are the colour indices, one obtains from formula (9)

$$C^{\alpha_1 \dots \alpha_4} = \frac{1}{36} \langle \Psi_c^{\{1\}} | \hat{\lambda}_1^{\alpha_1} \hat{\lambda}_2^{\alpha_2} [\hat{\lambda}_1^{\alpha_3} \hat{\lambda}_2^{\alpha_4} + \hat{\lambda}_3^{\alpha_3} \hat{\lambda}_1^{\alpha_4} + \hat{\lambda}_2^{\alpha_3} \hat{\lambda}_3^{\alpha_4} - \hat{\lambda}_2^{\alpha_3} \hat{\lambda}_1^{\alpha_4} - \hat{\lambda}_1^{\alpha_3} \hat{\lambda}_3^{\alpha_4} - \hat{\lambda}_3^{\alpha_3} \hat{\lambda}_2^{\alpha_4}] | \Psi_c^{\{1\}} \rangle. \quad (A.1)$$

Expression for $\bar{C}^{\alpha_1 \dots \alpha_4}$ after substitution $\hat{\lambda} \rightarrow \hat{\lambda}^T$ to formula (11) takes a form

$$\bar{C}^{\alpha_1 \dots \alpha_4} = \frac{1}{36} \langle \Psi_c^{\{1\}} | [\hat{\lambda}_1^{\alpha_3} \hat{\lambda}_2^{\alpha_4} + \hat{\lambda}_3^{\alpha_3} \hat{\lambda}_1^{\alpha_4} + \hat{\lambda}_2^{\alpha_3} \hat{\lambda}_3^{\alpha_4} - \hat{\lambda}_2^{\alpha_3} \hat{\lambda}_1^{\alpha_4} - \hat{\lambda}_1^{\alpha_3} \hat{\lambda}_3^{\alpha_4} - \hat{\lambda}_3^{\alpha_3} \hat{\lambda}_2^{\alpha_4}] \hat{\lambda}_1^{\alpha_1} \hat{\lambda}_2^{\alpha_2} | \Psi_c^{\{1\}} \rangle. \quad (A.2)$$

After substitution of (A.1), (A.2) into (11) an expression containing 36 terms arised. But only seven terms are independent

$$C_1 = (1212)(2121)$$

$$C_2 = (1212)(1221)$$

$$C_3 = (1231)(1321)$$

$$C_4 = (1231)(3112)$$

$$C_5 = (1231)(3121)$$

$$C_6 = (1212)(1321)$$

$$C_7 = (1212)(2321).$$

Here we use the abbreviation $(i_1 i_2 i_3 i_4)(j_1 j_2 j_3 j_4) \equiv$

$$\frac{1}{6^4} \sum_{\alpha_1 \dots \alpha_4=1}^8 \langle \Psi_c^{\{1\}} | \hat{\lambda}_{i_1}^{\alpha_1} \hat{\lambda}_{i_2}^{\alpha_2} \hat{\lambda}_{i_3}^{\alpha_3} \hat{\lambda}_{i_4}^{\alpha_4} | \Psi_c^{\{1\}} \rangle \langle \Psi_c^{\{1\}} | \hat{\lambda}_{j_1}^{\alpha_1} \hat{\lambda}_{j_2}^{\alpha_2} \hat{\lambda}_{j_3}^{\alpha_3} \hat{\lambda}_{j_4}^{\alpha_4} | \Psi_c^{\{1\}} \rangle.$$

The factor C in (11) is related to terms $C_1 \div C_7$ by the expression

$$C = 2C_1 - 2C_2 + 4C_3 + 4C_4 - 8C_5 + 8C_6 - 8C_7. \quad (A.3)$$

In calculation of the terms $C_1 \div C_7$ we use the Firz identity $\sum_{\alpha=1}^8 (\hat{\lambda}^\alpha)_k^i (\hat{\lambda}^\alpha)_m^n = -\frac{2}{3} \delta_k^i \delta_m^n + 2 \delta_m^i \delta_k^n$.

It gives a possibility to sum over indices $\alpha_1, \dots, \alpha_4$ in expressions for $C_1 \div C_7$. To sum over the colour indices of quarks we use the

$$\langle i_1 i_2 i_3 | \Psi_c^{[1]} \rangle = \frac{1}{\sqrt{6}} \varepsilon_{i_1 i_2 i_3}$$

After cumbersome calculations of $C_1 \div C_7$ we obtain from (A.3) the value of $C = 160/9$.

REFERENCES

1. Cohen-Tannoudji G., Hassouni A.E., Kalinowski J., Peschanski R. Phys.Rev., 1979, D19, p.3397.
2. Kaidalov A.B. JETP Lett., 1980, 32, p.494.
3. Kaidalov A.B. Phys.Lett., 1982, 116B, p.459.
4. Kaidalov A.B. In:"Elementary Particles",ITEP X School of Physics, M., Energoizdat, 1983.
5. Capella A., Tran Thanh Van J. Phys.Lett., 1982, 114B, p.450.
6. Kaidalov A.B., Ter-Martirosyan K.A. Yad.Fiz., 1984, 39, p.1545.
7. Kaidalov A.B., Ter-Martirosyan K.A. Yad.Fiz., 1984, 40, p.211.
8. Veselov A.I., Piskunova O.I., Ter-Martirosyan K.A. Phys.Lett., 1985, 158B, p.175.
9. Veneziano G. Phys.Lett., 1974, 52B, p.220.
Veneziano G. Nucl.Phys., 1974, B74, p.365.
10. Veneziano G. Nucl.Phys., 1976, B117, p.519.
11. Low F.E. Phys.Rev., 1975, D12, p.163.
12. Casher A., Neuberger H., Nussinov S., Phys.Rev., 1979, D20, 179.
13. Gurvich E.G. Phys.Lett., 1979, 87B, 386.
14. Chew G.F., Rosenzweig C. Phys.Rep., 1978, 41, p.264.
15. Rossi G.C., Veneziano G. Nucl.Phys., 1977, B123, p.507.
16. Rossi G.C., Veneziano G. Phys.Rep., 1980, 63, p.149.
17. Artry V. Nucl.Phys., 1975, B85, p.442.
18. Eilon Y., Harrari H. Nucl.Phys., 1974, B80, p.349.
19. Lee H. Phys.Rev.Lett., 1973, 30, p.719.
20. Veneziano G. Phys.Lett., 1973, 43B, p.413.
21. Chew G.F., Pignotti A. Phys.Rev., 1968, 176, p.2112.
22. Webber B.R. Nucl.Phys., 1976, B117, p.445.
23. Rushbroock J.G., Webber B.R. Phys.Rep., 1978, 44, p.1.
24. Volkovitsky P.E. Yad.Fiz., 1986, 43, p.268.
25. Kopeliovich B.Z. JINR, E2-86-471, Dubna, 1986.
26. Gunion J.F., Soper D.E. Phys.Rev., 1977, D15, p.2617.
27. Levin E.M., Ryskin M.G. Yad.Fiz., 1981, 34, p.1441.
28. Betman P. G, Laperashvili L.V. Yad.Fiz., 1985, 41, p.463.
Dorokhov A.E., Kochelev N.I. JINR, E2-86-224, Dubna, 1986.
29. Abbot L.F., Berger E.L., Blakenbecler R., Kane G.L., Phys.Lett., 1979, 88B, p.157.
30. Fredriksson S. et al. Z.Phys.C, 1982, 14, p.35.
31. Fredriksson S. et al. Z.Phys. c, 1983, 19, p.53.
32. Fredriksson S., Larsson T.I. Phys.Rev., 1983, D28, p.255.
33. Laperashvili L.V. Yad.Fiz., 1982, 35, p.742.
34. Breakstone A. et al. Z.Phys. C, 1985, 28, p.235.
35. Kim V.T., JINR, E2-87-75, Dubna, 1987.
36. Efremov A.V., Kim V.T. JINR, E2-87-74, Dubna, 1987.
37. Kobzarev I., Kondratyuk L., Martemyanov B, Schepkin M. Preprint ITEP, 86-67, Moscow, 1986.
38. Bronzan J.B., Sugar R.L. Phys.Rev., 1978, D17, p.2813.
39. Kuraev E.A., Lipatov L.N., Fadin V.S. JETP, 1977, 79, p.377.
40. Kopeliovich B.Z., Nikolaev N.N., Potashnikova I.K. JINR, E2-86-125, Dubna, 1986.
41. Camilleri L., Phys.Rep., 1987, 53, p.144.

Received by Published Department
on July, 15.

SUBJECT CATEGORIES OF THE JINR PUBLICATIONS

Index	Subject
1.	High energy experimental physics
2.	High energy theoretical physics
3.	Low energy experimental physics
4.	Low energy theoretical physics
5.	Mathematics
6.	Nuclear spectroscopy and radiochemistry
7.	Heavy ion physics
8.	Cryogenics
9.	Accelerators
10.	Automatization of data processing
11.	Computing mathematics and technique
12.	Chemistry
13.	Experimental techniques and methods
14.	Solid state physics. Liquids
15.	Experimental physics of nuclear reactions at low energies
16.	Health physics. Shieldings
17.	Theory of condensed matter
18.	Applied researches
19.	Biophysics

Копелцович Б.З., Захаров Б.Г. E2-84-548
 Аннигиляция антипротонов в дуальной партонной модели
 и теории возмущений КХД

В теории возмущений КХД вычислен вклад в сечение $\bar{p}p$ аннигиляции, обусловленный обменом двумя глюонами в декуплетном по цвету состоянии. Величина сечения существенно зависит от размера дикуарка в протоне и составляет около 1-2 мбн. Этот вклад слабо зависит от энергии и определяет сечение аннигиляции в асимптотике. Рассмотрен также механизм аннигиляции, доминирующий в преасимптотической области $\sqrt{s} < 12$ ГэВ/, где сечение быстро падает с энергией $\sim 1/\sqrt{s}$.

Работа выполнена в Лаборатории ядерных проблем ОИЯИ.

Препринт Объединенного института ядерных исследований. Дубна 1987

Kopeliovich B.Z., Zakharov B.G. E2-84-548
 Antiproton Annihilation in Dual Parton Model
 and Perturbative QCD

In the framework of perturbative QCD the contribution to the annihilation cross section resulting from exchange of two gluons in the colour decuplet state is calculated. The result depends essentially on the diquark radius, and is equal to 1+2 mb. This contribution slightly varies with energy and dominates the annihilation cross section in the asymptotics. The preasymptotical mechanism of annihilation is also considered which causes fast decrease in the cross section with energy ($\sim 1/\sqrt{s}$) at the intermediate energies $\sqrt{s} < 12$ GeV.

The investigation has been performed at the Laboratory of Nuclear Problems, JINR.

Preprint of the Joint Institute for Nuclear Research. Dubna 1987